SUPPLEMENTAL DATA

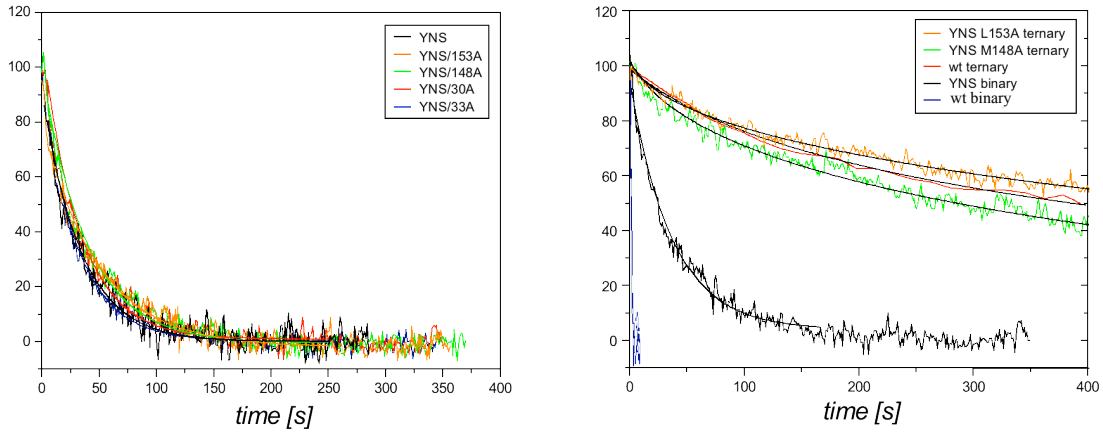

SUPPLEMENTAL FIGURE S1: *Ternary complex formation on artificial membranes*. **A.** Comparison of the dissociation of different IFNα2 YNS mutants from IFNAR1-H10 only fitted by a monoexponential dissociation model. **B.** Dissociation from the ternary complex for the mutants IFNα2-YNS/153A and IFNα2-YNS/148A in comparison to IFNα2 wt (taken from (26)). For comparison, the dissociation kinetics from IFNAR1 alone is shown for IFNα2-YNS and IFNα2 wt.

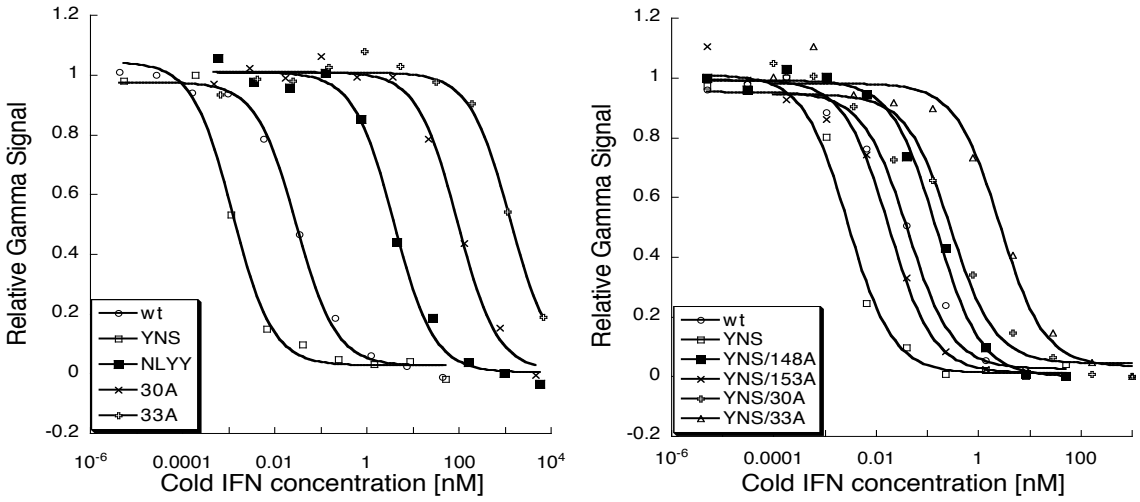

SUPPLEMENTAL FIGURE S2: *In situ binding inhibition curves of the different IFN mutants.* Signal emitted from I^{125}-labeled wild type IFNα2 was measured after competing with the tested IFNs at different concentrations (see experimental procedures). X-axis: interferon concentration; Y-axis: gamma signal of bound I125-labeled wild type IFNα2.

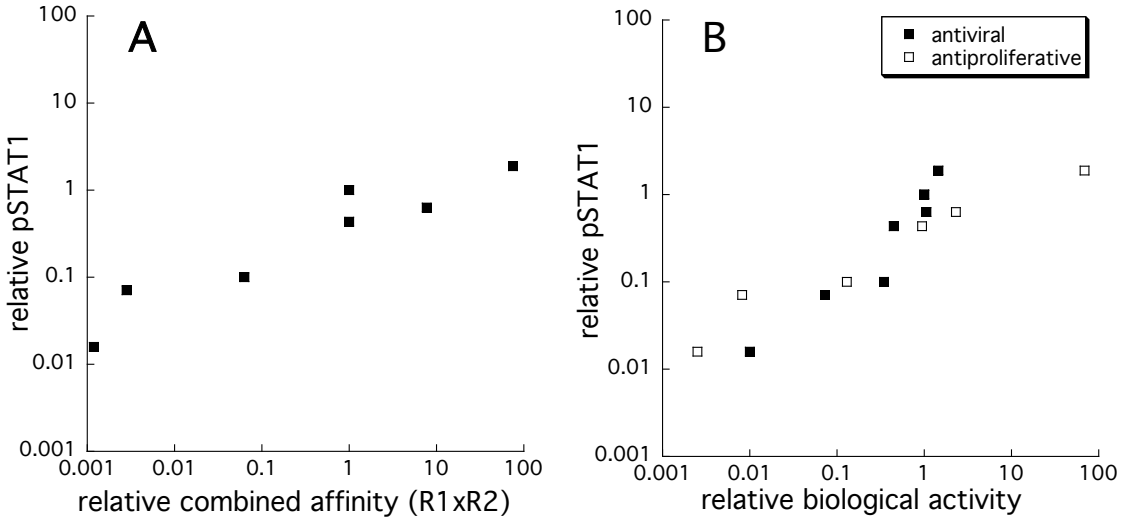

SUPPLEMENTAL FIGURE S3: *Relation between biological activities and pSTAT1*. **A**. pSTAT1 as a function of the combined affinity (R1xR2). **B**. Biological activity versus pSTAT1. Data were taken from Tables 2 and 3. All values are relative to wild-type.

SUPPLEMENTAL SCHEME 1: rate of accumulation of pSTAT1.

$$r1 + i \Leftrightarrow r1i$$

$$r2 + i \Leftrightarrow r2i$$

$$r1i + r2 \Leftrightarrow r1r2i$$

$$r2i + r1 \Leftrightarrow r1r2i$$

$$r1r2i \Leftrightarrow r1r2i_p$$

$$r1r2i_p + STAT1 \rightarrow r1r2i_p + pSTAT1$$

$$r1r2i \rightarrow D$$

To further quantify the STAT1 phosphorylation pattern, we simulated the rate of accumulation of pSTAT1 in cells using the Pro-Kineticist II software (Applied Photophysics Ltd., England). In the scheme $r1$ and $r2$ are the two receptors, i is interferon and $r1r2i_p$ is the active ternary complex. As input, we used the known concentrations of all proteins in the various experiments and the measured rate constants for the different interferon mutants as given in Tables 1-3. We assumed that the rate of dissociation of either one of the receptors from the ternary complex is the same as measured for the binary complex, and that the observed stabilization effect of the ternary complex (shown in figure 1) relates to a fast equilibrium between the binary and ternary complexes on the membrane (which is simulated in this model from the experimentally observed dissociation rates). We also assumed that the ternary complex ($r1r2i$) has to be activated (by Tyk2), and de-activated by either SOCS or receptor endocytosis (designated as D).